94-31

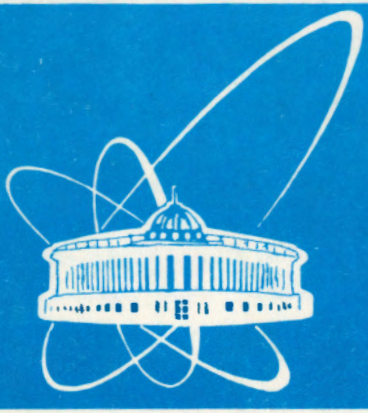

объединенный
институт
ядерных
исследований
дубна

E17-94-31

P.Vansant[1], F.M.Peeters[1],
M.A.Smondyrev[2], J.T.Devreese[3]

THE ONE-DIMENSIONAL BIPOLARON IN THE STRONG COUPLING LIMIT

Submitted to «Physical Review B»

---

[1]Departement Natuurkunde, Universitaire Instelling Antwerpen (UIA), Antwerpen, België

[2]On leave of absence: TUE, Eindhoven, Nederland

[3]Technische Universiteit Eindhoven, Eindhoven, Nederland
Permanent address: Departement Natuurkunde, Universitaire Instelling Antwerpen (UIA), Antwerpen, België; also at: Universiteit Antwerpen (RUCA), Antwerpen, België

1994

I. INTRODUCTION

Two electrons in a polar or ionic crystal will interact with each other through: 1) the direct *repulsive* Coulomb interaction, and 2) an *attractive* interaction caused by the polarization of the surrounding lattice. If the Coulomb interaction is sufficiently screened by the lattice and if the polaron interaction is sufficiently strong a bound state between the two electrons and the surrounding common cloud of virtual phonons may be formed. Such a composite quasi-particle is referred to as a *bipolaron.* One distinguishes the so-called *small* and *large* bipolarons, depending on whether the corresponding single polarons are in a localized state or are mobile, although with a large effective mass.

Earlier papers of Vinetskii[1], Mukhomorov[2], Suprun and Moizhes[3] obtained large stability regions for the bipolaron using a Coulombic type of wavefunction for each electron. Adamowski[4] and later Bassani et al.[5] used also variational calculations but compared the bipolaron ground state energy with more correct single polaron energies. Verbist, Smondyrev, Peeters and Devreese[6,7] used Feynman path-integral techniques and obtained more accurate results.

The study of bipolarons can be relevant to examine the applicability of the bipolaron theory to high-T_c superconductivity (e.g. for high-T_c superconductors[8,9], the recent discovered fullerites[10,11] and the proposed Bose-Einstein condensation of large bipolarons[12,13]).

It is interesting also to study relatively simple systems (for which the numerical work is greatly symplified) such as 1D bipolarons which could be relevant in quantum wires[14] and linear conjugated organic polymer conductors[15] where charges move in one dimension. In Ref. 16 it was recently proven that in the limit of a very strong magnetic field the 3D bipolaron maps into a 1D bipolaron problem.

The aim of the present paper is to present a more accurate and detailed treatment of 1D bipolaron formation in the strong-coupling limit. In this limit the adiabatic approximation leads to exact equations because the electron oscillations have a much larger frequency than the lattice frequency ω_{LO}. We will consider several characteristics of one 1D bipolaron, like e.g. the stability region which is found to be much larger in 1D than in 2D or 3D.

With the Fourier series approach we are also able to investigate the excited states of the 1D bipolaron. First of all, the relaxed excited states (RES) which are self-consistent solutions to the non-linear Schrödinger equation. The polarization is then adapted to the final electronic configuration. On the other hand, we have excited states which are the excited states in an effective potential well generated

by one of those self-consistent solutions (ground state or RES). For those excited states the polarization remains at the initial electronic configuration. The RES and Franck-Condon states of single polarons in 3D were studied by Devreese, Evrard and Kartheuser[17]. For their role on the surface of a liquid-helium film see Ref. 18.

The paper is organized as follows. In Sec. II we introduce the non-linear Schrödinger equation for the 1D bipolaron. This integro-differential equation is solved variationally in Sec. III and by a Fourier series expansion in Sec. IV. In the latter also a comparison is made of estimates for the ground state energy, the critical ratio $\eta_c, \ldots$, calculated within the two approaches. In Sec. V we investigate the excited states of the 1D bipolaron and in Sec. VI the conclusions are given.

II. STRONG-COUPLING LIMIT

The one-dimensional bipolaron Hamiltonian, which is the Hamiltonian of two electrons interacting with a phonon field, is given by

$$H = \sum_{j=1,2} \frac{p_j^2}{2m} + U(z_1 - z_2) + \sum_k \hbar\omega_k b_k^\dagger b_k + \sum_{j=1,2} \sum_k \left[V_k b_k e^{ikz_j} + \text{h.c.} \right], \qquad (2.1)$$

where z_j and p_j are the position and momentum operators of the j^{th} electron ($j = 1, 2$), m is the electron band mass and ω_k is the frequency of the phonons with wavevector k.

In the case of an electron interacting with the LO-mode we have dispersionless phonons $\omega_k = \omega_{LO}$ and the interaction coefficients are

$$V_k = -i\hbar\omega_{LO}\sqrt{\frac{2\alpha'}{L}}\sqrt{\frac{\hbar}{2m\omega_{LO}}} \qquad (2.2)$$

with L the length of the system and α' the coupling constant for the one-dimensional electron-phonon interaction (defined in Ref. 19 and 20)

$$\alpha' = \alpha\sqrt{\pi}\frac{\Gamma((D-1)/2)}{2\Gamma(D/2)}. \qquad (2.3)$$

Here α is the standard dimensionless electron-phonon coupling constant in 3D and D the number of space dimensions. For $D \to 1$ we have $\alpha' = \alpha/(D-1)$. Indeed, the polaron characteristics diverge for $D = 1$ because of the Coulombic nature of this problem. By using the renormalized coupling constant α' rather than α, all expressions are regularized and finite results are found for the energy and the mass of a polaron or bipolaron in 1D[19].

The 3D Coulomb repulsion between the electrons is defined by

$$\frac{U}{r} = U_D' \frac{\Gamma(D/2)}{\pi^{D/2+1}} \int \frac{\mathrm{d}^D\mathrm{k}}{k^{D-1}} \exp[i\mathrm{kr}],$$

$$U_D' = U\sqrt{\pi}\frac{\Gamma((D-1)/2)}{2\Gamma(D/2)} \qquad (2.4)$$

with $D = 3$. In the limit $D \to 1$ the corresponding Coulomb potential takes the form $2U_1'\delta(z_1 - z_2)$. This so-called contact potential is the natural generalization to 1D of the direct Coulomb repulsion between electrons in 3D. Therefore we have in (2.1) $U(z_1 - z_2) = 2U_1'\delta(z_1 - z_2)$. It is convenient to introduce also the dimensionless coupling constant U'

$$U_1' = \hbar\omega_{LO}\sqrt{\frac{\hbar}{m\omega_{LO}}}U' \qquad (2.5)$$

and the ratio of the coupling constants

$$g = \frac{U'}{\alpha'} = \frac{\sqrt{2}}{1-\eta}, \qquad (2.6)$$

where $\eta = \varepsilon_\infty/\varepsilon_0$ with $\varepsilon_\infty(\varepsilon_0)$ the high frequency (static) dielectric constant.

Starting from the Hamiltonian (2.1) we obtain in the strong coupling limit using the adiabatic approximation the non-linear effective Schrödinger equation of the one-dimensional bipolaron (for more details see Ref. 21)

$$\left\{ \frac{p_1^2}{2m} + \frac{p_2^2}{2m} + U(z_1, z_2; \Psi_0) \right\} \Psi_0(z_1, z_2) = E_0 \Psi_0(z_1, z_2) \qquad (2.7)$$

with the effective potential

$$U(z_1, z_2; \Psi_0) = U(|z_1 - z_2|) + 4\sum_k \frac{|V_k|^2 |\rho_k|^2}{\hbar\omega_k} - 2\sum_k \frac{|V_k|^2}{\hbar\omega_k} \left[\rho_k^* \left(e^{ikz_1} + e^{ikz_2} \right) + \text{c.c.} \right], \qquad (2.8)$$

in which the Fourier transform of the electron density is given by

$$\rho_k = \frac{\langle e^{ikz_1} \rangle + \langle e^{ikz_2} \rangle}{2} = \int_{-\infty}^{\infty} dz_1 dz_2 \left(\frac{e^{ikz_1} + e^{ikz_2}}{2} \right) \Psi_0^*(z_1, z_2) \Psi_0(z_1, z_2), \qquad (2.9)$$

the Coulomb repulsion

$$U(|z_1 - z_2|) = \hbar\omega_{LO}\sqrt{\frac{\hbar}{m\omega_{LO}}}\, 2U'\delta(z_1 - z_2) \tag{2.10}$$

and where the bipolaron wave function is normalized as follows

$$\int_{-\infty}^{\infty} dz_1 dz_2 \Psi_0^2(z_1, z_2) = 1, \tag{2.11}$$

To simplify the formulas we perform the following scaling $z_i \rightarrow \lambda z_i$, $(i = 1, 2)$ with

$$\lambda = \frac{1}{\alpha'}\sqrt{\frac{\hbar}{m\omega_{LO}}}\,, \tag{2.12}$$

which scales also the wavefunction Ψ_0

$$\Psi_0(\lambda z_1, \lambda z_2) = \frac{1}{\lambda}\chi(z_1, z_2)\,; \tag{2.13}$$

such that $\chi(z_1, z_2)$ is normalized to unity.

Finally we introduce

$$A = \frac{E_0}{\hbar\omega_{LO}\alpha'^2}\,, \tag{2.14}$$

which leads to the non-linear effective Schrödinger equation (see Appendix A)

$$\left\{-\frac{1}{2}\frac{\partial^2}{\partial z_1^2} - \frac{1}{2}\frac{\partial^2}{\partial z_2^2} + \tilde{U}(z_1, z_2; \chi)\right\}\chi(z_1, z_2) = A\,\chi(z_1, z_2) \tag{2.15}$$

with

$$\begin{aligned}
&\tilde{U}(z_1, z_2; \chi) = \\
&\sqrt{2}\int_{-\infty}^{\infty} dx_1 dx_2 dx_2'\, \chi^2(x_1, x_2)\chi^2(x_1, x_2') + \sqrt{2}\int_{-\infty}^{\infty} dx_1 dx_1' dx_2\, \chi^2(x_1, x_2)\chi^2(x_1', x_2) - \\
&2\sqrt{2}\int_{-\infty}^{\infty} dx_2' \left[\chi^2(z_1, x_2') + \chi^2(z_2, x_2')\right] - 2\sqrt{2}\int_{-\infty}^{\infty} dx_1' \left[\chi^2(x_1', z_1) + \chi^2(x_1', z_2)\right] + \\
&2g\delta(z_1 - z_2) + 2\sqrt{2}\int_{-\infty}^{\infty} dx_1 dx_1' dx_2\, \chi^2(x_1, x_2)\chi^2(x_1', x_1).
\end{aligned} \tag{2.16}$$

III. THE VARIATIONAL APPROACH

By multiplying both sides of (2.15) with $\chi(z_1, z_2)$ and after integration over z_1 and z_2 the above integro-differential equation (2.15) can be rewritten as a variational problem. The ground state energy can then be obtained from the minimalization of the functional

$$\begin{aligned}
&F[\chi] = \frac{1}{2}\int_{-\infty}^{\infty} dz_1 dz_2 \left(\frac{\partial\chi(z_1, z_2)}{\partial z_1}\right)^2 + \frac{1}{2}\int_{-\infty}^{\infty} dz_1 dz_2 \left(\frac{\partial\chi(z_1, z_2)}{\partial z_2}\right)^2 + \\
&2g\int_{-\infty}^{\infty} dz\, \chi^2(z, z) - 2\sqrt{2}\int_{-\infty}^{\infty} dz_1 dz_1' dz_2\, \chi^2(z_1, z_2)\chi^2(z_1', z_1) - \\
&\sqrt{2}\int_{-\infty}^{\infty} dz_1 dz_2 dz_2'\, \chi^2(z_1, z_2)\chi^2(z_1, z_2') - \sqrt{2}\int_{-\infty}^{\infty} dz_1 dz_1' dz_2\, \chi^2(z_1, z_2)\chi^2(z_1', z_2).
\end{aligned} \tag{3.1}$$

with respect to $\chi(z_1, z_2)$.

Gross[22] showed that the analogous strong coupling 1D polaron problem could be solved exactly in the adiabatic approximation (see also Ref. 23). Therefore we can obtain exact results if $\alpha \rightarrow \infty$. In this case of the 1D polaron the energy functional, in dimensionless units and analogue to (3.1), is

$$F_1[\phi] = \frac{1}{2}\int_{-\infty}^{\infty} dz \left(\frac{\partial\phi(z)}{\partial z}\right)^2 - \sqrt{2}\int_{-\infty}^{\infty} dz\, \phi^4(z). \tag{3.2}$$

and the exact ground state wave function was found to be

$$\phi(z) = \frac{1}{2^{1/4}\cosh\sqrt{2}(z - z_0)}, \tag{3.3}$$

with the exact binding energy $E_1^{exact} = -1/3$ in units of $\hbar\omega_{LO}\alpha'^2$. Notice that this result corresponds to the one of Ref. 22 when we apply the scaling $z \rightarrow 2z$ and do not take into account the second term in Eq. (3.2) which equals 5/24 and shifts the zero-point energy. When a Gaussian trial wave function $\Psi = (2b/\pi)^{1/4}\exp(-bx^2)$ is chosen[19] the energy is $E_1^{gauss} = -1/\pi$ with the variational parameter $b = 1/\pi$.

To investigate the bipolaron energy it seems natural to use a superposition of two 1D polaron wavefunctions. Thus the trial wave function is constructed as a symmetrical ($\epsilon = 1$) or antisymmetrical ($\epsilon = -1$) combination of two 1D polaron wave functions

$$\chi_0(b,d;z_1,z_2) =$$

$$\frac{bN}{2}\left[\frac{1}{\cosh b(z_1-z_{10})\cosh b(z_2-z_{20})}+\frac{\epsilon}{\cosh b(z_2-z_{10})\cosh b(z_1-z_{20})}\right], \qquad (3.4)$$

with the normalization $N=1/\sqrt{2(1+\epsilon\, d^2/\sinh^2 d)}$ and $d=b(z_{10}-z_{20})$ in which the z_{i0} are the polaron positions. Here b is a variational parameter which is a measure of the inverse width of the individual electron wave functions and d is a variational parameter which describes the separation or distance between the two polarons. Because of the translation invariance of the system all results will depend on the relative average distance between the polarons rather than on the single polaron positions z_{10} and z_{20}. Inserting Eq. (3.4) into Eq. (3.1) and performing the scaling $z_i \to z_i/b$, we obtain the following bipolaron energy

$$A[\chi_0] = b^2 T - b(U_1 - gU_2), \qquad (3.5)$$

with the kinetic term

$$T=\int_{-\infty}^{\infty} dz_1 dz_2 \left(\frac{\partial\chi_0(1,d;z_1,z_2)}{\partial z_1}\right)^2, \qquad (3.6)$$

the electron-phonon selfenergy

$$U_1 = 4\sqrt{2}\int_{-\infty}^{\infty} dz_1 dz_2 dz_2'\ \chi_0^2(1,d;z_1,z_2)\chi_0^2(1,d;z_1,z_2'), \qquad (3.7)$$

and the Coulomb repulsion

$$U_2 = 2\int_{-\infty}^{\infty} dz\ \chi_0^2(1,d;z,z). \qquad (3.8)$$

Notice that the minimalization of Eq. (3.5) with respect to b becomes very simple and leads to the energy

$$A(d) = -\frac{[U_1-gU_2]^2}{4T}, \qquad (3.9)$$

with the variational parameter $b=(U_1-gU_2)/2T$ and the physical condition $U_1 - gU_2 \geq 0$.

For a symmetrical bipolaron wave function the bipolaron energy functional $A(d)$ is shown in Fig. 1 as function of the relative distance d between the two electrons

for different values of $g = U'/\alpha'$: the relative strength of the Coulomb repulsion versus the electron-phonon coupling. Notice that $A(d)$ is an even function of d and therefore only the region $d \geq 0$ is shown. Furthermore, the physical region corresponds to $\eta > 0$ which implies $g = U'/\alpha' > \sqrt{2}$. For completness we have also shown the curves for $g < \sqrt{2}$ in Fig. 1. At large d, the bipolaron energy tends to the limit $A_{\max} = -2/3$, which is twice the energy of a single polaron as it should be. In the absence of electron-electron repulsion, i.e. $U' = 0$, the minimum is reached at $d = 0$ and the energy is $A(0) = -8/3$. In the latter case the wave function (3.4) takes the form

$$\chi_0 = \frac{\sqrt{2}}{\cosh 2\sqrt{2}(z_1-z_0)\cosh 2\sqrt{2}(z_2-z_0)}, \qquad (3.10)$$

which indeed is the solution of Eq. (2.15) for $U' = 0$. In Fig. 2a the bipolaron energy is shown as a function of g and Fig. 2b depicts the corresponding separation d_{eq} between the two polarons. For $g < g_c = 1.782$ the minimum of the bipolaron energy is reached at a finite value of d. However, for $g > g_c$ $A(d)$ atains its minimum energy for $d = \infty$ which implies that the bipolaron state is unstable and two separate polarons are formed. This critical value g_c corresponds to $\eta = 0.206$.

For the antisymmetrical bipolaron wave function ($\epsilon = -1$) we have $A(d) > A_{\max} = -2/3$ for any value of d and g, which implies that the bipolaron state will decompose into two separate polarons. In fact, even for $g = 0$ it was found that $A(d)$ obtains its maximum at $d = 0$ with $A(0) = -416/735 \approx -0.56599$, which is 15% larger than the energy of two separated polarons. This result seems to indicate the instability of the 1D bipolaron excited state. Obviously, an improved variational wavefunction may lead to a different conclusion.

To improve the above variational estimates it is convenient to introduce the center-of-mass coordinates

$$Z = \frac{z_1+z_2}{2}, \qquad P = p_1 + p_2, \qquad (3.11)$$

and the relative coordinates

$$z = z_1 - z_2, \qquad p = \frac{p_1 - p_2}{2}. \qquad (3.12)$$

We use the notation $\chi(z_1,z_2) = \Psi(Z,z)$ and the symmetry $|\chi(z_1,z_2)|^2 = |\chi(z_2,z_1)|^2$ of the wave function. The variational problem (3.1) then takes the following form

$$A[\Psi] = \frac{1}{4}\int_{-\infty}^{\infty} dZ dz \left(\frac{\partial\Psi(Z,z)}{\partial Z}\right)^2 + \int_{-\infty}^{\infty} dZ dz \left(\frac{\partial\Psi(Z,z)}{\partial z}\right)^2 -$$

$$4\sqrt{2}\int_{-\infty}^{\infty}dZdzdz'\Psi^2(Z,z)\Psi^2(Z+z/2,z')+2g\int_{-\infty}^{\infty}dZ\Psi^2(Z,0). \qquad (3.13)$$

It is well-known that in the asymptotical limit of the strong coupling limit the adiabatic approximation becomes exact, and therefore we consider the following product-wave function Ansatz

$$\Psi(Z,z)=\Phi(Z)\phi(z). \qquad (3.14)$$

Following Ref. 7 we take for the center-of-mass wave function

$$\Phi(Z)=\left[\frac{\omega\alpha'^2}{2\pi}\right]^{1/4}\exp(-\frac{\omega\alpha'^2Z^2}{4}), \qquad (3.15)$$

which leads to the following functional

$$A[\phi]=\frac{\omega}{16}+\omega\int_{-\infty}^{\infty}\left(\frac{d\phi}{dz}\right)^2dz+2\sqrt{2\omega}\left[\frac{\phi^2(0)}{1-\eta}-\right.$$
$$\left.\frac{1}{\pi}\int_{-\infty}^{\infty}dz_1dz_2\exp\left(-\frac{(z_1+z_2)^2}{16}\right)\phi^2(z_1)\phi^2(z_2)\right] \qquad (3.16)$$

with ω a variational parameter. The ground state bipolaron energy E_{bip} (in units of $\hbar\omega_{LO}\alpha'^2$) is then obtained by minimalizing the functional $A[\phi]$ with respect to ω and ϕ.

The bipolaron can exist as a stable state when the binding energy $|E_{bip}|$ is larger than twice the single polaron energy $|E_1|$. In the strong coupling limit $|E_{bip}|\sim\alpha'^2$ and $|E_1|\sim\alpha'^2$, and as a consequence α'^2 can be factored out. The bipolaron formation is then exclusively determined by the physical parameter η. It is found that a critical value η_c exists below which a bipolaron state will be energetically more favorable than a state with two single polarons.

Of course the condition for bipolaron formation will depend on the value of E_1 (E_1^{exact} or E_1^{gauss}) which we choose (see e.g. Ref. 7). The corresponding η_c will be denoted by η_c^{exact} for $E_1=E_1^{exact}=-1/3$ and η_c^{approx} for $E_1=E_1^{gauss}=-1/\pi$. The η_c^{exact} is a lower bound to η_c, due to the fact that the obtained bipolaron energy is an upper bound to the exact energy. For η_c^{approx} is it neither an upper bound nor a lower bound. Both η_c values are given in this paper. Normally, one should compair the bipolaron energy with twice the energy of the single polaron obtained within the same approximation. However, in this case the exact single polaron energy E_1^{exact} is available. Therefore, we can obtain with E_1^{exact} a lower bound to η_c .

The dependence of the wave function on the relative coordinates is contained in $\phi(z)$ for which we choose:

$$1)\ \phi(z)=N(1+B|z|)\exp(-\frac{\nu|z|}{2}), \qquad (3.17a)$$
$$2)\ \phi(z)=N(1+B|z|+Cz^2)\exp(-\frac{\nu|z|}{2}), \qquad (3.17b)$$
$$3)\ \phi(z)=N(1+Cz^2)\exp(-\frac{\nu^2z^2}{4}), \qquad (3.17c)$$
$$4)\ \phi(z)=N(1+Cz^2+Dz^4)\exp(-\frac{\nu^2z^2}{4}), \qquad (3.17d)$$
$$5)\ \phi(z)=N(1+B|z|)\exp(-\frac{\nu^2z^2}{4}), \qquad (3.17e)$$
$$6)\ \phi(z)=N(1+B|z|+Cz^2)\exp(-\frac{\nu^2z^2}{4}), \qquad (3.17f)$$

where N is the normalization constant and B, C, D and ν are variational parameters.

In contrast to the 2D and 3D cases, the direct Coulomb repulsion in 1D is a contact potential, which implies that for the 1D bipolaron ground state: a) the wave function $\phi(z)$ is not zero for $z=0$, and b) the first derivative of $\phi(z)$ can be discontinuous at $z=0$. Therefore, the constant term in the polynomial part of $\phi(z)$ is not negligible as it was in 2D and 3D (see Ref. 7).

In Fig. 3 the bipolaron groundstate energy, in units of $\hbar\omega_{LO}\alpha'^2$, is plotted as a function of η for all the above trial functions. These energy values are also given in Table I for a selective number of η-values. We observe that: a) the trial function (6) gives the best results (i.e. the lowest upper bound), b) these results are close to the results of trial function (5), c) the term $B|z|$ in the wavefunction turns out to be very important as can be seen by comparing the results from trial wave functions (3) and (4) which do not contain this linear term in z, with the result of trial wave function (5) and (6), and d) it is surprising that the exponential decreasing functions (1) and (2) give smaller binding energies than the best Gaussian function (6). The opposite is true for the single polaron case[19]. The two dashed horizontal lines in Fig. 3 correspond to twice the single polaron energy calculated using the asymptotical exact wavefunction (3.3) and a Gaussian respectively. The crossings of the ground state bipolaron energy curves with those straight lines determine the critical η_c-value at which bipolaron formation occurs. These values of η_c are listed in Table II for the different variational wavefunctions. The trial function (6) gives the lowest bipolaron ground state energy and consequently the largest η_c value. Because the η_c^{exact} are lower bounds to η_c, is the largest η_c^{exact} obtained with trial function (6) the best lower bound for η_c within the variational approach.

The critical (minimal) value of the electron-phonon coupling constant α'_c is determined by the condition $E^{bip}(\alpha'_c, U') = 2E^{pol}(\alpha'_c)$ that the bipolaron ground state energy equals the ground state energy of two independent free polarons. Using the Feynman path-integral technique this value was found to be $\alpha_c = 6.8$ for the 3D case[6]. It was proven that within this path-integral approach the polaron[24,25] and bipolaron[6] ground state energies satisfy scaling relations such that the corresponding energies in nD can be obtained from the one in 3D. Applying these scaling relations one obtains[16] $\alpha'_c = 2.3$ in 1D.

Earlier works[5–7] already indicated an enlargement of the stability region for bipolaron formation in low-dimensional systems as compared to 3D systems. From the values for η_c^{approx}, η_c^{exact} and α'_c (see Fig. 3 and Table III) we find that the bipolaron stability region is even more enlarged in the 1D case, in comparison with the stability region in 2D or 3D.

We will now concentrate on the trial function (6), Eq. (3.17f), which gives the lowest bipolaron ground state energy of all trial wavefunctions. The results for the energy could be fitted to the curve $E = -1.07 + 0.737\eta - 0.273\eta^2$, within 1.5% over the range $\eta \in [0, 0.9]$. The $|\phi(z)|^2$ of the resulting wave function is shown in Fig. 4a for different values of η. We observe the increased separation of the two polarons with increasing η, i.e. increasing Coulomb repulsion. Notice also that: 1) with decreasing value of η the electrons are on average much closer to each other, 2) $|\phi(z=0)|^2$ is non-zero, and 3) $\partial\phi(z)/\partial z$ is discontinuous at $z = 0$. This is different in 2D and 3D where $|\phi(z=0)|^2 = 0$ and $\partial\phi(z)/\partial z$ are continuous at $z = 0$. In Fig. 4b we plot this $|\phi(z)|^2$ for $\eta = 0.5$ together with the corresponding function for the single polaron.

The rms separation (in units of $\sqrt{\hbar/m\omega_{LO}\alpha'^2}$) between the electrons is defined by

$$R = [\langle z^2 \rangle]^{1/2}, \tag{3.18}$$

where the averaging is performed over the trial wavefunctions of Eqs. (3.17). The evolution of R as a function of η is shown in Fig. 5 for the different trial functions. Notice that R increases with increasing repulsion, η, as expected. For the "best" trial wavefunctions this increase is a smooth function of η. For the trial function (6), Eq. (3.17f), we found $R(\eta = 0) = 2.53$ and $R(\eta = \eta_c^{exact} = 0.764) = 3.35$.

IV. THE FOURIER SERIES APPROACH

The power of the variational approach lies in the fact that the method provides an upper bound to the bipolaron binding energy. This gives a criterium to judge

which is the best bipolaron wavefunction. On the other hand, it is less clear how to improve in a systematic way on a given variational wavefunction. In the variational approximation of Sec. III also an exponential form for the center-of-mass wavefunction (3.15) was examined but it was found that this does not improve our results. Another way is to include more terms in the series expansion. But, the fact that adding a term in the polynomial of Eq. (3.17e) does not lower substantially the bipolaron energy (less than 0.4%) may be an indication that the resulting bipolaron wavefunction, Eq. (3.17f), is close to the exact result. Because this is not a guarantee that this is also the case, we will present below a different approach which inherently allows for systematically improving the bipolaron binding energy. Furthermore, this method allows to calculate besides the ground state, also excited states. A second advantage will be that we do not have to make the product ansatz approximation (3.14).

Using the symmetry of the wave function $|\chi(z_1, z_2)|^2 = |\chi(z_2, z_1)|^2$ which allows as well the symmetric as the antisymmetric solution, we obtain for the non-linear effective Schrödinger equation (2.15)

$$\left\{-\frac{1}{2}\frac{\partial^2}{\partial z_1^2} - \frac{1}{2}\frac{\partial^2}{\partial z_2^2} + \tilde{U}(z_1, z_2; \chi)\right\}\chi(z_1, z_2) = A\chi(z_1, z_2) \tag{4.1}$$

with

$$\tilde{U}(z_1, z_2; \chi) = 4\sqrt{2}\int_{-\infty}^{\infty} dx_1 dx_2 dx'_2 \chi^2(x_1, x_2)\chi^2(x_1, x'_2) - 4\sqrt{2}\int_{-\infty}^{\infty} dx'_2 \left[\chi^2(z_1, x'_2) + \chi^2(z_2, x'_2)\right] + 2g\delta(z_1 - z_2). \tag{4.2}$$

Next we interpret the potential (4.2) as given and solve (4.1) numerically. In order to do so we put our system in a square box with dimension $[-L, L]$ and infinite high wells. The bipolaron wavefunction can now be written as a linear combination of the basisfunctions of this box

$$\chi(z_1, z_2) = \sum_{n,m}^{N,M} a_{nm} \sin\frac{n\pi(z_1 + L)}{2L} \sin\frac{m\pi(z_2 + L)}{2L}. \tag{4.3}$$

Multiply both sides of equation (4.1) with $\chi(z_1, z_2)$ and integrate over z_1 and z_2. The resulting equation is an eigenvalue problem which provides us the binding energy and the parameters a_{nm} for a given potential $\tilde{U}$. Because this potential $\tilde{U}$ depends on the wavefunction χ in a non-linear way we consequently solve the problem iteratively by

inserting the found wavefunction into $\hat{U}$ until convergence is obtained. In principle this is an exact procedure when $N = M = \infty$. In practice, because of limite computer memory, we have to limit ourselves to a finite number of terms in Eq. (4.3), typically $N = M = 15$. By systematically increasing the number of terms we will find better upper bounds to the bipolaron energy.

The resulting η_c^{exact} value for $N = M = 15$ is given in Table II. Using the symmetry of the ground state in the program we had the possibility to calculate the ground state bipolaron energies E_{FS} for some discrete values of η with $N = M = 30$. They are tabulated in Table I.

Notice that this method gives higher ground state energies, and thus lower binding energies, as compared to the best variational solution. Therefore we investigate the dependence of the bipolaron energy on the number of Fourier terms in our expansion (4.3). The result is shown in Fig. 6 for $\eta = 0.5$. We found that the numerical data (solid dots) could be well presented by the curve (solid curve in Fig. 6) $E_{bip} = E_0 - B/n$ with $E_0 = -0.783$ and $B = -0.965$ for $\eta = 0.5$. This is a very slowly converging series with n which explains why we found less accurate binding energies as compared to the variational approach. Therefore we used the fit $E_{bip} = E_0 - B/n$ in order to obtain the $n = N = M \rightarrow \infty$ results of the Fourier expansion which are also given in Table I. These ground state energies are also indicated in Fig. 3 by stars which we were able to fit to the polynomial: $E = -1.176 + 1.062\eta - 0.551\eta^2$ with an accuracy of 4% in the region $\eta \in [0, 0.9]$. We see that these energies E_{FS}^{∞} are lower than the variational results and go asymptotically to the energy of two single polarons. The prove of this statement is explained in the next section. The corresponding η_c^{exact} is in this case 1.0. Therefore, the ground state is always stable and will exist.

In Fig. 7 the wavefunction $\chi(z_1, z_2)$ together with its contourplot are shown for $\eta = 0.5$ and $N = M = 15$. From this figure it is clear that the two electrons avoid each other and that they have the highest probability to be at a certain distance from each other. In order to make a direct comparison between the best variational wavefunction, Eq. (3.17f), and the one obtained with the Fourier series, Eq. (4.3), we show in Fig. 8 for $\eta = 0.5$ the respective electron probabilities as function of: (a) the relative position between the two electrons

$$\phi^2(z) = \int_{-\infty}^{\infty} dZ\ \chi^2(z, Z)\,; \tag{4.4}$$

and (b) the center-of-mass coordinate of the two electron system. The latter is defined similar as Eq. (4.4) but now we integrate over the relative coordinate z.

Notice that: 1) in the variational approach the electron wavefunction for $\eta = 0.5$ falls off faster as compared to the Fourier series approach, and this both as a function of the relative coordinate and as function of the center-of-mass coordinate; 2) the electrons are on the average further from each other in the Fourier series method; and 3) the translational motions are very close to each other.

The rms separation R (3.18) between the two electrons is also shown in Fig. 5. for the Fourier series approach (stars). Notice that for $\eta < 0.35$ the Fourier series approach predicts that the electrons are less far separated as compared to the best variational approach. For $\eta > 0.35$ the opposite is true and the difference between the two approaches increases with increasing η (see also Fig. 8).

Within the strong coupling limit the effective bipolaron mass is given by (see Ref. 21)

$$\frac{m^*}{m} = 2 + 8\sqrt{2}\alpha^{4} \int_{-\infty}^{\infty} dz_1 dz_2 dz_2' \left[\frac{\partial}{\partial z_1}\chi^2(z_1, z_2)\right]\left[\frac{\partial}{\partial z_1}\chi^2(z_1, z_2')\right]. \tag{4.5}$$

In Fig. 9 the results of the electron-phonon correction to the bipolaron mass $\Delta m^*/m = m^*/m - 2$ is shown for the best variational wavefunction (dashed curve) and for the Fourier series approach (points) with $N = M = 15$ and $\eta = 0.5$. We observe that in the limit of large η the variational approach reproduces almost the correct asymptotical value of two separated 1D polarons (dashed line). From this figure we also can conclude that the Fourier series approach is not accurate enough to obtain good estimates for the energy and the effective mass. As mentioned earlier, for the energy we can extrapolate an accurate result, but for the wave function we can't do this. Therefore the effective mass which is calculated with this wave function is not so accurate within the Fourier series approach.

Another important quantity of interest is the effective bipolaron potential (4.2) which we consider without the constant term and the δ-function term. This δ-function term only would cause a discontinuous value at $z = 0$ and the constant term only determines the zero-point energy level. The effective bipolaron potential is shown in Fig. 10 as function of the relative position $z = z_1 - z_2$ of the two electrons for the best variational function (dashed curve) and for the Fourier series approach (solid curve). Notice that: 1) the potential becomes zero for large $|z|$ which is a consequence of the fact that the effect of the interaction between the electrons vanishes for large distances, 2) the effective potential within the variational approach is more localized and deeper than the one of the Fourier series approach, 3) the derivative of the considered potential is discontinuous at $z = 0$ which is a

consequence of the δ-function repulsion at $z = 0$, and 4) the potential has two local minima which correspond to the average separation between the two electrons.

In the numerical scheme of the Fourier series approach the energy converges much faster than the wave function. Because of this and the limitations in computer time the wave function did not converge yet in the numerical calculations with $N = M = 30$. Therefore, we used in the calculations of the rms separation, the effective mass and the effective potential (in which calculations we use the wave function) the Fourier series approach with $N = M = 15$.

V. THE EXCITED STATES

With the Fourier series approach we are also able to investigate the excited states of the 1D bipolaron, namely: the relaxed excited states (RES) which are self-consistent solutions to the non-linear Schrödinger equation and the excited states in an effective potential well generated by one of the self-consistent solutions. In what follows we use the quantum number $n \geq 1$ to enumerate the self-consistent solutions and $n' \geq 1$ to enumerate the excited states in an effective potential well generated by one of the self-consistent solutions. Therefore, $\varepsilon_{n,n'}$ will be the energy of the n'-th state in the effective potential generated by the n-th self-consistent solution.

In Table IV the energies $\varepsilon_{n,n'}$ are listed for $n = 1 \div 4$ and $n' = 1 \div 4$ for a bipolaron in a box with length $2L = 7$. Those energies are calculated with $N = M = 15$. The diagonal elements $\varepsilon_{n,n}$ in Table IV are the energies of the groundstate ($n = 1$) and of the first, second and third RES states ($n = 2, 3, 4$). They correspond to the self-consistent solutions for which the polarization is adapted to the final electronic configuration. Indeed, in the case of a RES with quantum number n the effective potential is calculated every iteration with the eigen-function corresponding to the n^{th} eigenvalue obtained in the iteration before.

If we consider the energies of the excited states in an effective potential well generated by e.g. the first RES, namely $\varepsilon_{2,n'}$, and confined to a box with length $2L = 7$, we see from Table IV that the state with $n' < n = 2$, namely $n = 2$ and $n' = 1$, has a considerably lower energy than the energy $\varepsilon_{2,2}$ of the RES. This phenomenon is even more clear for $n = 3$ (see Table IV). We have then two states with lower energies as the RES. The reason for this behaviour are the symmetry properties of those states. The first RES, for instance, has an antisymmetric wave function which is a self-consistent solution to the Schrödinger equation. In this case the effective potential is generated by the RES itself. In the latter potential we can

look for excited states. The first one ($n = n' = 2$) corresponds then to the RES. It is indeed antisymmetric. The ground state in this potential ($n = 2$ and $n' = 1$) is however symmetric and has therefore a lower energy. Even more, from the ground state energy $E_{pol} = -0.332$ of the 1D polaron[26] in a box with length $2L = 7$, and from the value $\varepsilon_{2,1} = -0.679$ (see Table IV), we can conclude that this state is stable and will exist for certain values of the box length $2L$ and η (see also later). Higher excited states have, of course, larger energies (see Table IV).

For the energies of the excited states as function of the box length $2L$ we have practically the same behaviour as in the case of the 1D-polaron in a box[26]. Indeed, the energies of the excited states $\varepsilon_{n,n'}$ with $n' \leq n$ all converge to the energy $\varepsilon_{n,n}$ of the RES when we increase the box length $2L$. Nevertheless, there is an important difference: In the limit of an infinitely large box we found that the excited states are grouped because of symmetry reasons. Therefore, we obtain e.g. for the states in the potential well generated by the first RES groups existing of two energy levels (see Fig. 11). Apparently, the $\varepsilon_{n,n'}$ consist of groups of $n + 1$ energy levels if $n = 3$, and of n energy levels if $n = 2$. In Fig. 12 we plot the energy spectrum for $n \leq 3$ and $n' \leq n + 1$ ($n = 3$) or $n' \leq n$ ($n = 1, 2$). For $n = 3$ it gives the first part of the spectrum of the bipolaron in the potential generated by the second RES. The energies $\varepsilon_{3,n'}$ for $n' \leq 4$ as function of the box length $2L$ show us that in the limit of an infinitely large box the energy levels indeed combine to groups as discussed above and that in this limit all these energies $\varepsilon_{3,n'}$ ($n' \leq 4$) tend to the energy $E_{RES2} = \varepsilon_{3,3}$ of the second RES. This energy level is then 4 fold degenerated. This degeneracy of the RES energy at large box length is caused by the possible symmetry of the wave functions in that case. In Fig. 13 we plot those wave functions for $n = 3$, $n' \leq 4$ and $2L = 19$. They correspond to the energies $\varepsilon_{3,1}$ (a), $\varepsilon_{3,2}$ (b), $\varepsilon_{3,3}$ (c) and $\varepsilon_{3,4}$ (d). We see the four symmetries obtained by combinating the symmetry relations $\chi(z_1, z_2) = \pm\chi(z_2, z_1)$ and $\chi(z_1, z_2) = \pm\chi(-z_1, -z_2)$ which are allowed by the integro-differential equation (2.15).

For the excited states in the potential generated by the first RES the symmetry relations are restricted to the two combinations: $\chi(z_1, z_2) = \chi(z_2, z_1)$ and $\chi(z_1, z_2) = \chi(-z_1, -z_2)$, and $\chi(z_1, z_2) = -\chi(z_2, z_1)$ and $\chi(z_1, z_2) = -\chi(-z_1, -z_2)$. This explains the grouping seen in Fig. 11 and 12.

With $\eta = 0.2$ the numerical results for the energies of the ground state and the first three RES states in the limit of an infinitely large box and an infinite number of terms in the Fourier series ($N = M \to \infty$) are respectively: $\varepsilon_{1,1} = -0.986$, $\varepsilon_{2,2} = -0.667$, $\varepsilon_{3,3} = -0.442$ and $\varepsilon_{4,4} = -0.416$. The $\varepsilon_{n,n}$ with n even

correspond to an antisymmetrical wave function. In this case the δ-function does not contribute because the wave function is zero at $z_1 = z_2$. However, for the RES states with odd n the δ-function will play an important role. To understand better the structure of the bipolaron RES states we added in Appendix B a discussion about the relation between the 1D bipolaron and the single 1D polaron characteristics, especially concerning the energies and the symmetries of the corresponding wave functions.

In the same limits as for the above RES states the energies of the ground state, the first RES and the ground state in the potential of the first RES are shown in Fig. 14 as a function of η. The 1D bipolaron ground state is always stable and will exist. The first RES however has a constant energy $E_{RES1} = -0.667$ which corresponds to twice the single polaron energy. Because of this energy value for the first RES we see that the energy of the ground state (within the same limits) should be lower than this value -0.667. Taking into account that the ground state energy increases with increasing η and that the numerically obtained upperbound (within the same limits as above) tends to the same value for $\eta = 1.0$, we can conclude that in the limit of an infinite large box $\eta_c^{exact} = 1.0$.

In the potential generated by this first RES the ground state has a lower energy $\varepsilon_{2,1}$ which goes asymptotically to E_{RES1} when $\eta \to 1$ (infinitely separated electrons). Therefore, this state will be stable except in the case of an infinite high δ-function ($\eta \to 1$). Nevertheless, because the energy of the first RES equals twice the single polaron energy, the probability of finding two electrons in this first RES will be very small. To obtain the ground state in the potential generated by the first RES the electrons need to be situated firstly in the first RES itself from where this ground state can be reached. Therefore the probability to obtain this ground state in the potential generated by the first RES will also be very small despite of being stable.

VI. CONCLUSIONS

The 1D bipolaron ground state has been treated in the limit of strong electron-phonon coupling. We obtained the critical value α'_c of the effective electron-phonon coupling constant and lower bounds for the critical ratio η_c of the dielectric constants which determine the phase diagram for bipolaron formation at zero temperature. From those values we conclude that the stability region for bipolaron formation is much larger in 1D than in 2D and 3D. The most important characteristics of the 1D bipolaron, like the root mean squared distance between the electrons, the bipolaron mass and the effective potential were calculated.

Within the Fourier series approach it is straigthforward to obtain the possible excited states of the bipolaron. We found that the ground state will be bound and the first RES has an energy which equals the energy of two single polarons. The ground state in the potential generated by the first RES is however stable. Because of symmetry reasons the higher excited states combine to groups with the same energy when we consider the limit of an infinitely large box.

ACKNOWLEDGMENTS

M.A.S. is grateful to the University of Antwerp (UIA) and Eindhoven University of Technology for the support (NWO grant for visitors No. 07-13-137) and the kind hospitality during his visit to the Benelux. P.V. thanks the Belgian Science Foundation and the Joint Institute for Nuclear Research for the support of his visit to Dubna. This work is partly performed in the framework of "Diensten voor de Programmatie van het wetenschapsbeleid" (Belgium) under contract No. IT/SC/24, the supercomputerproject of the NFWO, the FKFO project 2.0093.91 and the ALPHA-project of NFWO-Universiteit Antwerpen.

APPENDIX A

The integro-differential equation (2.15) is central to the present paper and is obtained from (2.7). In the present paper we will give the intermediate steps to go from Eq. (2.8) to Eq. (2.15). When we consider only the optical phonons and substitute the expression for V_k into Eq. (2.8) we obtain

$$4\sum_k \frac{|V_k|^2\ |\rho_k|^2}{\hbar\omega_k} = \frac{2\alpha'\hbar}{\pi}\sqrt{\frac{2\hbar\omega_{LO}}{m}}\int_{-\infty}^{\infty} dk|\rho_k|^2. \qquad \text{(A1)}$$

Next we substitute ρ_k, as given by Eq. (2.9), in the integral, which results into

$$\int_{-\infty}^{\infty} dk|\rho_k|^2 = \frac{1}{4}\int_{-\infty}^{\infty} dx_1dx_2dx'_1dx'_2\ \Psi_0^2(x_1,x_2)\Psi_0^2(x'_1,x'_2)$$
$$\times \int_{-\infty}^{\infty} dk\left[e^{ik(x_1-x'_1)} + e^{ik(x_1-x'_2)} + e^{ik(x_2-x'_1)} + e^{ik(x_2-x'_2)}\right]$$

$$= 2\pi \int_{-\infty}^{\infty} dx_1 dx_2 dx_2' \Psi_0^2(x_1, x_2) \Psi_0^2(x_1, x_2'). \quad \text{(A2)}$$

where we used also the symmetry $\Psi_0^2(x_1, x_2) = \Psi_0^2(x_2, x_1)$. For the other term in Eq. (2.8) we have

$$\sum_k \frac{|V_k|^2}{\hbar\omega_k} \left[\rho_k^* \left(e^{ikx_1} + e^{ikx_2}\right) + \rho_k \left(e^{-ikx_1} + e^{-ikx_2}\right)\right]$$
$$= \frac{2\alpha'\hbar\omega_{LO}}{\sqrt{2m\hbar\omega_{LO}}} \frac{1}{2\pi} \int_{-\infty}^{\infty} dk \left[\rho_k^* \left(e^{ikx_1} + e^{ikx_2}\right) + \rho_k \left(e^{-ikx_1} + e^{-ikx_2}\right)\right]$$
$$= \frac{\alpha'}{2\pi} \frac{\sqrt{2\hbar\omega_{LO}}}{m} \int_{-\infty}^{\infty} dk \left[\rho_k^* \left(e^{ikx_1} + e^{ikx_2}\right) + \rho_k \left(e^{-ikx_1} + e^{-ikx_2}\right)\right]. \quad \text{(A3)}$$

As an example we calculate one integral of this expression

$$\int_{-\infty}^{\infty} dk\ \rho_k^* e^{ikz} = \frac{1}{2} \int_{-\infty}^{\infty} dx_1 dx_2\ \Psi_0^2(x_1, x_2) \int_{-\infty}^{\infty} dk \left[e^{ik(z-x_1)} + e^{ik(z-x_2)}\right]$$
$$= \pi \int_{-\infty}^{\infty} dx_1 dx_2\ \Psi_0^2(x_1, x_2) \left[\delta(z - x_1) + \delta(z - x_2)\right]$$
$$= \pi \int_{-\infty}^{\infty} dx_2\ \Psi_0^2(z, x_2) + \pi \int_{-\infty}^{\infty} dx_1\ \Psi_0^2(x_1, z). \quad \text{(A4)}$$

The other integrals in Eq. (A3) are calculated in a similar way. Substitute these results in Eq. (2.7), perform the scaling (2.12) and we obtain the integro-differential equation (2.15).

APPENDIX B

To better understand the structure of the bipolaron RES let us consider an unphysical situation when $g = 0$ that is when the delta-function repulsion potential in Eq. (2.16) is not taken into account. Two particles interacting with the common phonon field tend to combine together. But the effective potential becomes separable and a bipolaron wave function can be represented as a symmetrized or an antisymmetrized product of 'one-particle' wave functions:

$$\chi(z_1, z_2) = N[\chi_1(z_1)\chi_2(z_2) + \gamma\chi_1(z_2)\chi_2(z_1)], \quad \text{(B1)}$$

where $\gamma = 1$ (-1) for symmetrical (antisymmetrical) states and the normalization constant in Eq. (B1) is defined by the relation:

$$1 = 2N^2 \left[1 + \gamma \left(\int_{-L}^{L} dz\, \chi_1(z)\chi_2(z)\right)^2\right]. \quad \text{(B2)}$$

If both particles are in the same state, a bipolaron wave function is of the form:

$$\chi(z_1, z_2) = \chi(z_1)\chi(z_2). \quad \text{(B3)}$$

Note that such state is a symmetrical one under a permutation of particles $z_1 \leftrightarrow z_2$. Then the effective potential of Eq. (2.16) takes the form:

$$\tilde{U}(z_1, z_2; \chi) = \tilde{U}(z_1) + \tilde{U}(z_2)$$
$$\tilde{U}(z) = 2\sqrt{2} \int_{-L}^{L} dz\, \chi^4(z) - 4\sqrt{2}\chi^2(z), \quad \text{(B4)}$$

and the equation for the one-particle wave functions is as follows:

$$-\frac{1}{2}\chi''(z) + \tilde{U}(z)\chi(z) = \frac{A}{2}\chi(z). \quad \text{(B5)}$$

If we perform a scaling $z_{1(2)} \to z_{1(2)}/2$ and change the wave functions $\chi(z/2) = \sqrt{2}\phi(z)$ to preserve the normalization condition we obtain from Eq. (B5)

$$-\frac{\phi''(z)}{2} - 2\sqrt{2}\phi^3(z) + \phi(z)\sqrt{2}\int_{-2L}^{2L} dz \phi^4(z) = \frac{A}{8}\phi(z). \quad \text{(B6)}$$

The latter equation is nothing more than an analogous equation for a single polaron in a box of a double length $(-2L, 2L)$ so we can exploit the solutions found in Ref. 26 with $A/8$ playing the role of a polaron energy ϵ_{n_1} where n_1 is a number of a subsequent RES. The corresponding wave function of the RES (the so called cnoidal wave) has n_1 equidistant peaks, located at the points $z = L(2m - n_1 - 1)/n_1$, $m = 1, 2, \ldots, n_1$. It is symmetrical under reflections $(z \leftrightarrow -z)$ for odd n_1 and antisymmetrical for n_1 being even. Thus, the resulting bipolaron wave function constructed from the one-particle RES wave functions have n_1^2 peaks some of which are positive and others are negative. In the limit of an infinite large box $L \to \infty$ we've found for negative energies of a single polaron in a box the expression $\epsilon_{n_1} = -1/(3n_1^2)$ from which follow results for the bipolaron energies

$$A_{n_1,n_1} = -\frac{8}{3n_1^2}, \qquad n_1 = 1, 2, \ldots \tag{B7}$$

When the delta potential repulsion is switched on it contributes to the energy with a positive term so these levels will take higher values.

In particular, the bipolaron ground state ($n_1 = 1$) wave function at $g = 0$ has one peak at the point $z_1 = z_2 = 0$ and the ground state energy is $A_{1,1} = -8/3 \approx -2.667$. Because of the repulsion it is split into two peaks at a short distance and symmetrical to the line $z_1 = z_2$ as is shown in Fig. 7. The ground state energy becomes equal to $\epsilon_{1,1}$ shown in Fig. 3.

The symmetrical combination of the one-polaron first RES ($n_1 = 2$) has two positive peaks located at the points $z_1 = z_2 = \pm L/2$ and two negative peaks located at the points $z_1 = -z_2 = \pm L/2$. With the repulsion two peaks located on the line $z_2 = z_1$ should split into 4 so that the total number of peaks will be equal to 6. The energy of the state will be larger than it is at $g = 0$ (that is, larger than $A_{2,2} = -2/3 \approx -0.667$), so this state is unstable.

Remember that we deal for the moment with the bipolaron RES states, whose wave functions are constructed as (symmetrical) products of the *same* one particle RES wave functions. Inserting a general bipolaron wave function of Eq. (B1) into Eq. (4.1), (4.2) we arrive at the equations:

$$\begin{aligned} &\chi_1(z_1)\, D\chi_2(z_2) + \chi_2(z_2)\, D\chi_1(z_1) + \\ &\gamma\left[\chi_1(z_2)\, D\chi_2(z_1) + \chi_2(z_1)\, D\chi_1(z_2)\right] = 0, \end{aligned} \tag{B8}$$

where the operator D is defined as follows:

$$\begin{aligned} D\chi_i(z) = &-\frac{1}{2}\chi_i''(z) + \frac{U_\infty - A}{2}\chi_i(z) - \\ &4\sqrt{2}N^2\left[\chi_1^2(z) + \chi_2^2(z) + 2\gamma\,\chi_1(z)\,\chi_2(z)\int_{-L}^{L} dz'\,\chi_1(z')\,\chi_2(z')\right]\chi_i(z), \end{aligned} \tag{B9}$$

and the asymptotical value U_∞ of the effective potential (4.2) takes the form

$$\begin{aligned} U_\infty = 4\sqrt{2}N^4 \Bigg\{ &\int_{-L}^{L} dz\,[\chi_1^2(z) + \chi_2^2(z)]^2 + 4\int_{-L}^{L} dz\,\chi_1^2(z)\,\chi_2^2(z)\left(\int_{-L}^{L} dz\,\chi_1(z)\,\chi_2(z)\right)^2 + \\ &4\gamma\int_{-L}^{L} dz\,\chi_1(z)\,\chi_2(z)\,[\chi_1^2(z) + \chi_2^2(z)]\int_{-L}^{L} dz\,\chi_1(z)\,\chi_2(z)\Bigg\}. \end{aligned} \tag{B10}$$

Solutions to Eq. (B9) can be constructed with eigenvectors of the operator D:

$$D\chi_i(z) = C_i\,\chi_i(z). \tag{B11}$$

Inserting into Eq. (B9) we obtain that

$$C_1 + C_2 = 0. \tag{B12}$$

The important case is when the wave functions χ_1, χ_2 have different symmetries under reflections. Then the interception integral

$$\int_{-L}^{L} dz\chi_1(z)\,\chi_2(z) = 0$$

and formulae (B2), (B9), (B10) are simplified. The same occurs in the limit of an infinite large box when χ_1, χ_2 have peaks in different places, which are, of course, infinitely separated from each other.

As an example we suppose that $\chi_1(z)$ is a symmetrical function in z and $\chi_2(z)$ is an antisymmetrical function. Suppose also that being squared these functions will coincide in the limit of the infinitely large box. Then we have $N = 1/\sqrt{2}$ and obtain the following equations from Eq. (B9), (B10):

$$\begin{aligned} -\frac{1}{2}\chi_1''(z) + \tilde{U}(z)\,\chi_1(z) &= \left(\frac{A}{2} + C_1\right)\chi_1(z), \\ -\frac{1}{2}\chi_2''(z) + \tilde{U}(z)\,\chi_2(z) &= \left(\frac{A}{2} - C_1\right)\chi_2(z), \\ \tilde{U}(z) &= 2\sqrt{2}\int_{-L}^{L} dz\,\chi_1^4(z) - 4\sqrt{2}\,\chi_1^2(z). \end{aligned} \tag{B13}$$

Performing the same scaling as in Eq. (B5) we conclude that we can choose as χ_2, for example, the first RES of a single polaron, and as χ_1 — the excited polaron state which is the ground state in the potential generated by χ_2. Indeed these functions have the supposed symmetries under reflections and peaks at the points $z = \pm L/2$ which are infinitely separated in the limit $L \to \infty$. Thus we obtain from Eq. (B13):

$$\begin{aligned} \frac{A}{8} + \frac{C_1}{4} &= \epsilon^{(1)}_{2,1}, \\ \frac{A}{8} - \frac{C_1}{4} &= \epsilon^{(1)}_{2,2}, \end{aligned} \tag{B14}$$

where $\epsilon^{(1)}_{n_1,n_1'}$ is the single polaron energy in a state with the mentioned quantum numbers first of which is related to a RES and the second — to an excited state in

the potential of that RES. From Eq. (B12) and (B14) we obtain the expression for the energy of this bipolaron state in the limit of a large box:

$$A = 4\left(\epsilon_{2,1}^{(1)} + \epsilon_{2,2}^{(1)}\right) = -\frac{2}{3}. \qquad \text{(B15)}$$

The resulting bipolaron wave functions have two peaks (a positive and a negative) at the points $z_2 = z_1 = \pm L/2$ and $z_2 = -z_1 = \pm L/2$ for the symmetrical and antisymmetrical states, respectively. Two possible peaks similar to that of the state constructed earlier as a combination of RES states only are cancelled. Note that we constructed a bipolaron RES from a single polaron RES and the ground state in the potential generated by this RES. With the repulsion the peaks of the symmetrical state will be splitted and its energy takes a higher value. This state corresponds to $\epsilon_{3,3}$ (see Fig. 13). The antisymmetrical state is not influenced by the delta-function repulsion so its wave function and the energy is the same as was described. It corresponds to $\epsilon_{2,2}$ and is exactly the same as we obtained numerically.

There are other bipolaron RES states, but their energies are too high and therefore we do not consider them here.

TABLE I. The numerically calculated bipolaron energies, in units of $\hbar\omega_{LO}\alpha'^2$, for different values of η. We give the results $E(n)$ for the different trial functions (see Eq. (3.17)) and for the Fourier series approach E_{FS} ($N = M = 30$), E_{FS}^{∞} ($N = M \to \infty$).

η	$E(1)$	$E(2)$	$E(3)$	$E(4)$	$E(5)$	$E(6)$	E_{FS}	E_{FS}^{∞}
0.0	-1.008	-1.070	-0.935	-0.943	-1.067	-1.071	-1.071	-1.133
0.1	-0.938	-1.003	-0.852	-0.866	-1.002	-1.005	-1.001	-1.060
0.2	-0.868	-0.937	-0.777	-0.794	-0.938	-0.942	-0.932	-0.986
0.3	-0.801	-0.873	-0.713	-0.728	-0.876	-0.880	-0.865	-0.913
0.4	-0.738	-0.814	-0.665	-0.677	-0.820	-0.823	-0.805	-0.845
0.5	-0.681	-0.760	-0.641	-0.646	-0.769	-0.771	-0.751	-0.783
0.6	-0.631	-0.712	-0.633	-0.636	-0.725	-0.726	-0.705	-0.727
0.7	-0.587	-0.670	-0.627	-0.630	-0.688	-0.688	-0.674	-0.688
0.8	-0.550	-0.635	-0.622	-0.624	-0.656	-0.656	-0.656	-0.669
0.9	-0.518	-0.520	-0.613	-0.619	-0.610	-0.620	-0.648	-0.667

TABLE II. The critical η_c-values are given for all trial wavefunctions and for the Fourier series expansion (FS) with $N = M = 30$ and the extrapolated result with $N = M \to \infty$.

Trial function	η_c^{approx}	η_c^{exact}
1)	0.587	0.527
2)	0.796	0.710
3)	0.551	0.393
4)	0.595	0.424
5)	0.874	0.764
6)	0.874	0.764
FS (N=M=15)	----	0.672
FS($N = M \to \infty$)	----	1.000

TABLE III. The critical values α_c', η_c^{approx} and η_c^{exact} are given for 1D, 2D and 3D. In the case of 1D we consider the η_c as obtained: 1) with the best variational wavefunction and 2) the Fourier series approach (FS).

	α_c'	η_c^{approx}	η_c^{exact}
3D	6.8	0.131	0.119
2D	2.9	0.158	0.136
1D (var)	2.3	0.874	0.764
1D (FS)	2.3	—	0.672
1D (FS$^{\infty}$)	2.3	—	1.000

TABLE IV. The energy levels of the first four states ($n' = 1 \div 4$) in potentials generated by the four first RES states ($n = 1 \div 4$) for the 1D bipolaron in a box of the size $2L = 7$. The diagonal elements are the energies $\epsilon_{n,n}$ of the corresponding RES states.

$n \setminus n'$	1	2	3	4
1	-0.882	-0.324	0.294	0.502
2	-0,679	-0.646	0.231	0.369
3	-0.580	-0.405	-0.172	-0.082
4	-0.507	-0.343	-0.164	-0.093

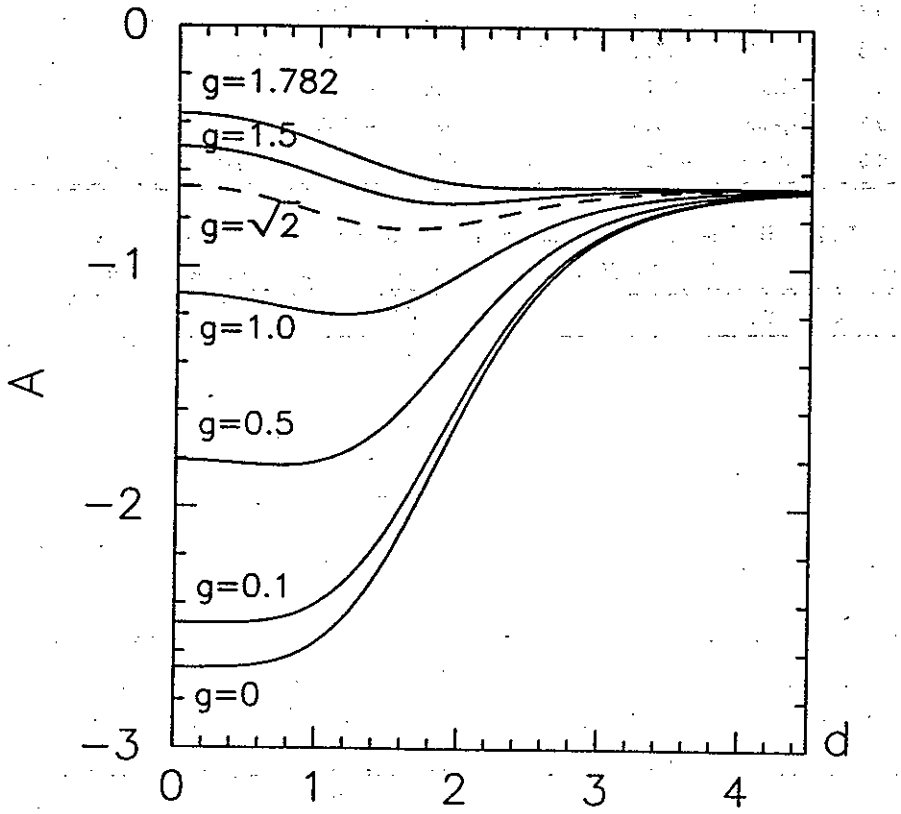

FIG. 1. Bipolaron energy functional $A(d)$ vs. the relative distance d between the electrons for the symmetrical trial wave function, Eq. (3.4) with $\epsilon = 1$, for different values of the direct Coulomb repulsion $g = U'/\alpha'$. The dashed curve corresponds to the limiting case $g = \sqrt{2}$ which divides the physical ($g < \sqrt{2}$) and the unphysical region ($g > \sqrt{2}$).

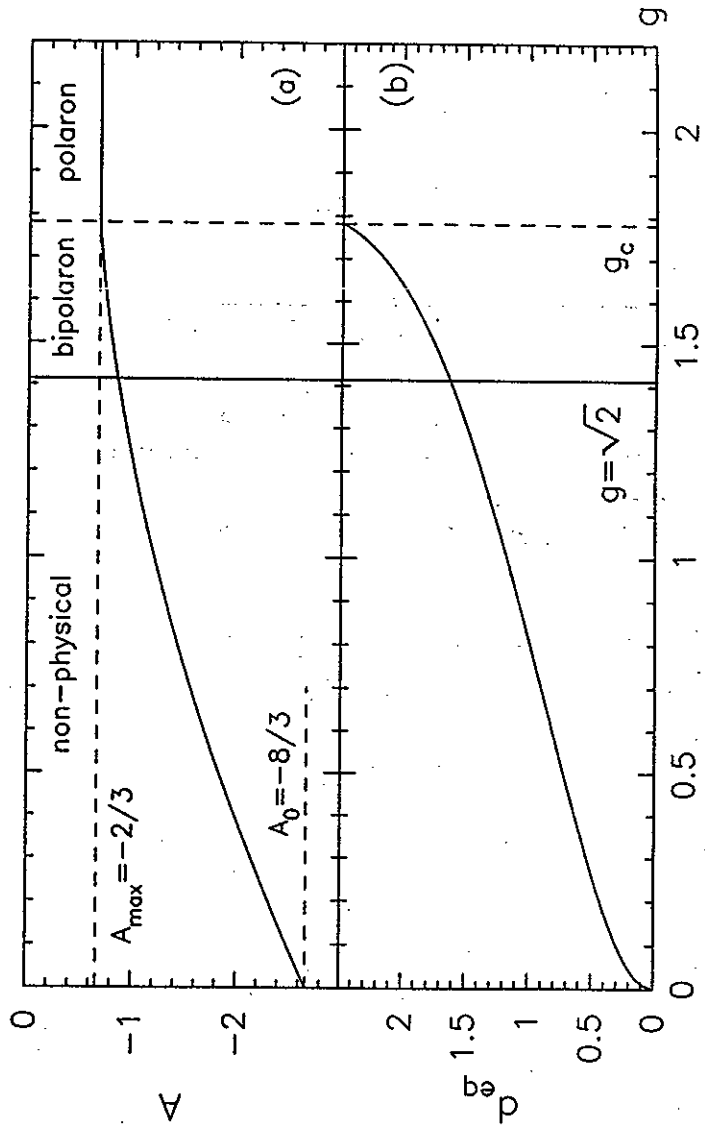

FIG. 2. (a) The bipolaron energy $A = E_{bip}/\hbar\omega_{LO}\alpha'^2$ as obtained by minimizing $A(d)$ (see Fig. 1) with respect to d vs. the dimensionless coupling constant g. At the critical value $g_c = 1.782$ the energy equals -2/3 which separates the stable bipolaron region from the unstable one where the bipolaron will decay into two separate polarons; (b) The equilibrium distance d_{eq} between the electrons as obtained by minimizing $A(d)$ (see Fig. 1) with respect to d is plotted vs. the coupling constant g.

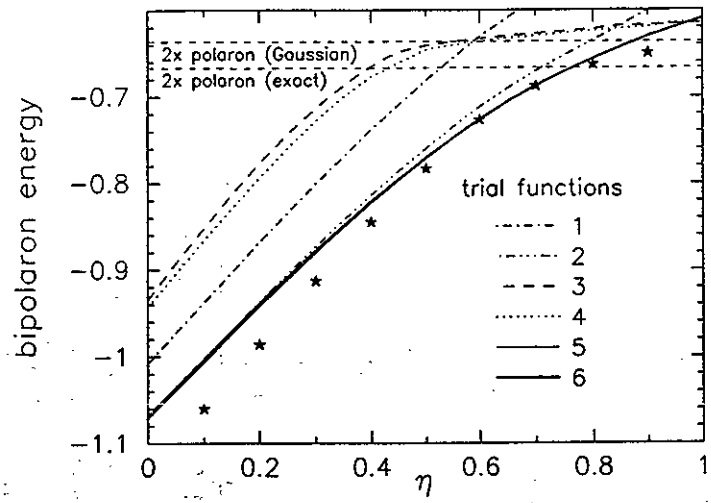

FIG. 3. The bipolaron energy is plotted vs. η for the six trial functions and for the solution of the integro-differential equation using the Fourier serie approach and extrapolating the $n \to \infty$ limit (stars). The horizontal lines give the energy of two separate polarons $E = 2E_1$ where: 1) E_1 is calculated within the Gaussian approach, and 2) E_1 is the exact result. The crossings of the curves with the straight lines determine the η_c values.

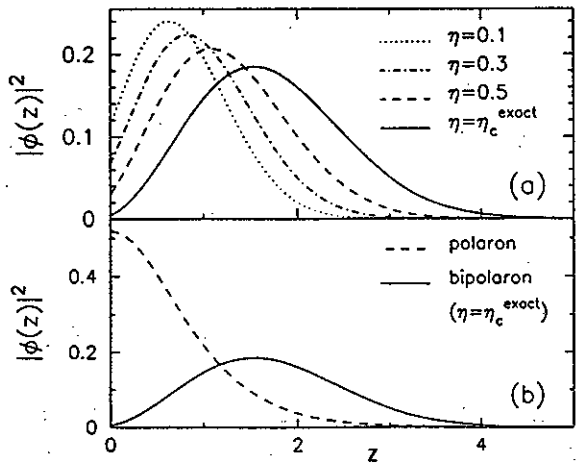

FIG. 4. For the best trial function 6 (see Eq. (3.17f)) we show: (a) the electron density within the bipolaron $|\phi(z)|^2$ as function of the relative separation between the two electrons for several values of η, and (b) for $\eta = 0.6$ this function is shown together with the electron density in the case of a single polaron.

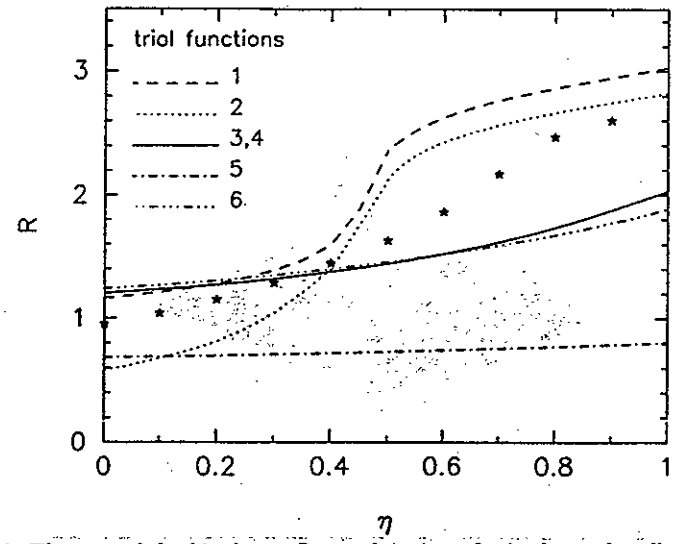

FIG. 5. The rms of the bipolaron R as a function of η is shown for all the considered trial functions and for the wave function obtained by the Fourier series approach (stars).

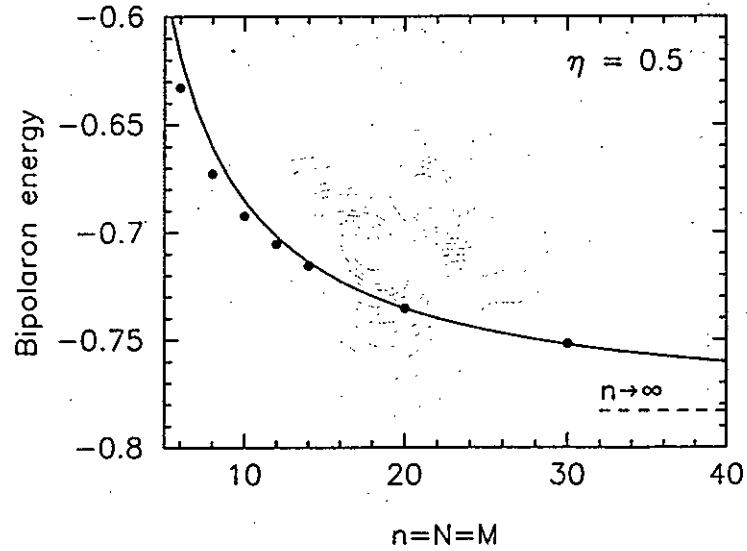

FIG. 6. The convergence of the numerical results for the ground state energy within the Fourier series approach is shown for $\eta = 0.5$ as function of $N = M = n$, the number of Fourier series components for each electron. The solid curve is given by $E_{bip} = E_0 - B/n$ where E_0 and B are determined by the $n = 20$ and $n = 30$ results.

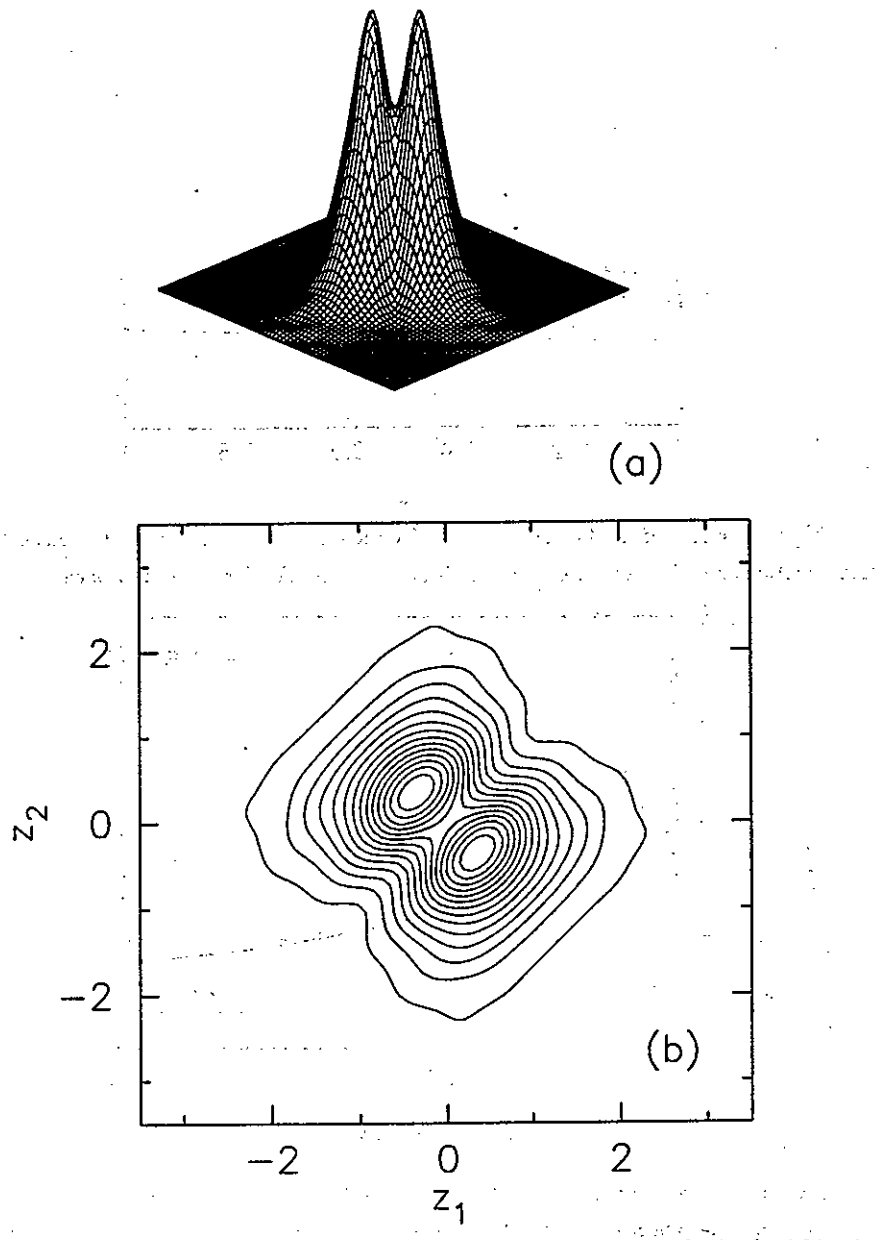

FIG. 7. (a) The bipolaron wavefunction $\phi(z_1, z_2)$ for $\eta = 0.2$ as obtained within the Fourier series approach. (b) The contour map corresponding to this bipolaron wavefunction.

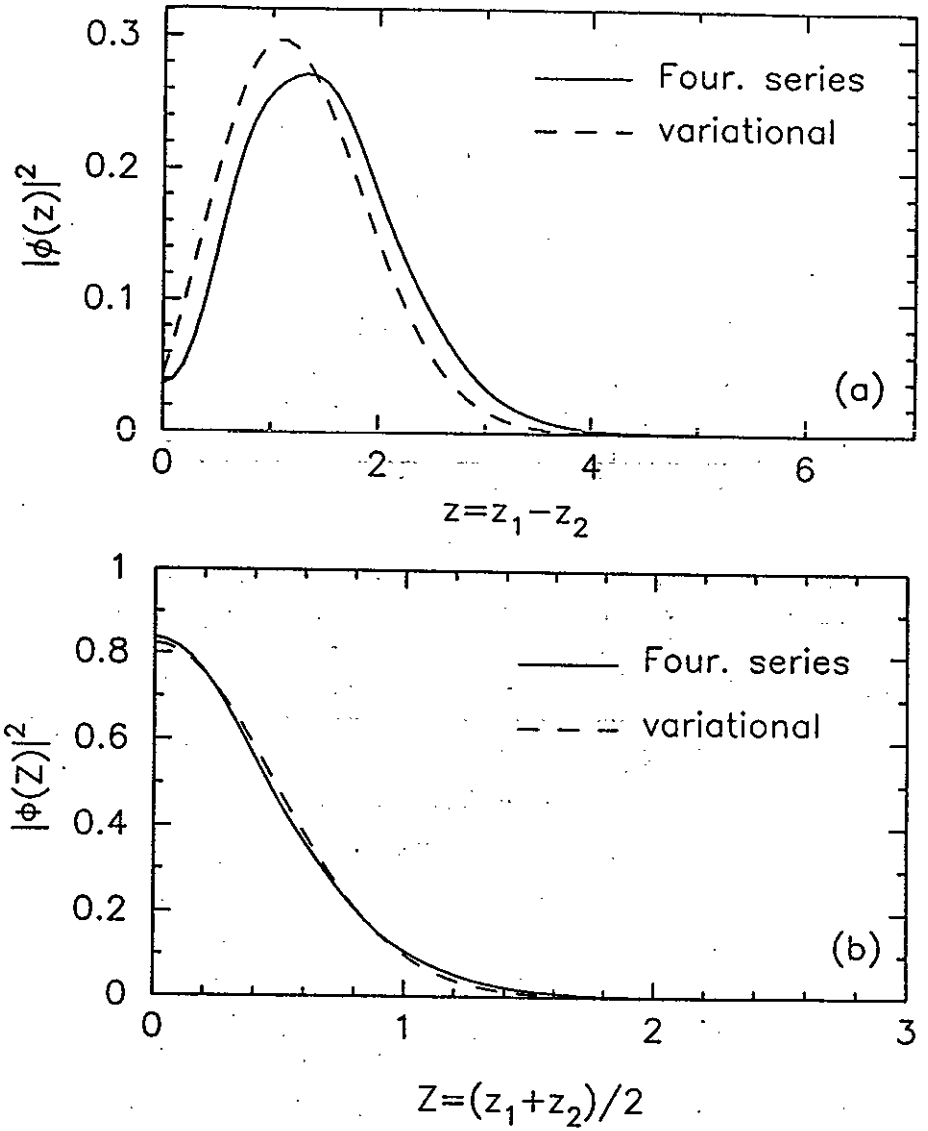

FIG. 8. The electron density within the bipolaron for $\eta = 0.5$ is given: (a) as function of the relative distance between the electrons, and (b) as function of the center-of-mass coordinate. We compare the results from the Fourier series approach (solid curves) and from the best variational wavefunction (dashed curves).

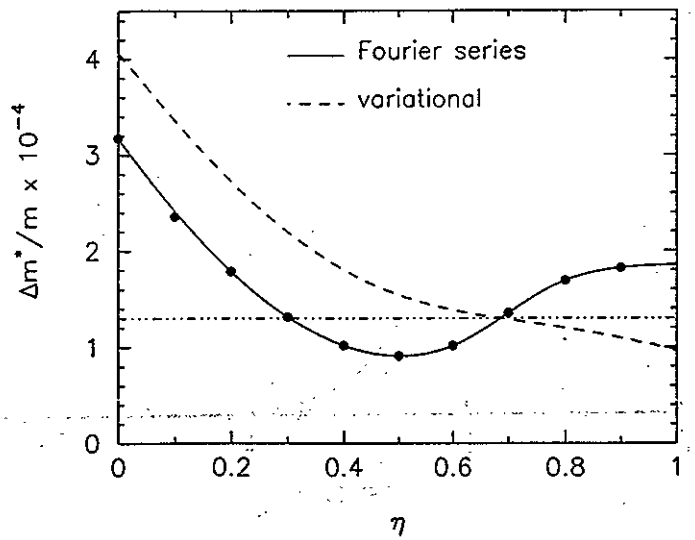

FIG. 9. The electron-phonon correction to the effective mass as obtained within the variational approach (dashed line) and within the Fourier series approach (points). The solid curve is only a fit true those numerical data. The horizontal line indicates the value of two times the effective mass of a strongly coupled 1D polaron.

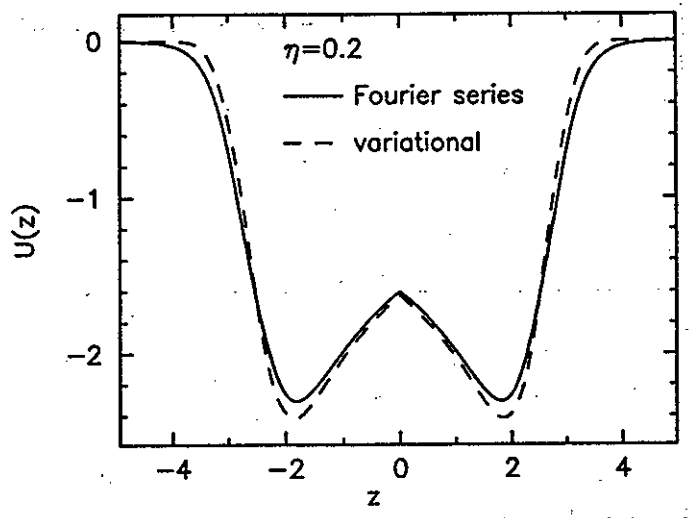

FIG. 10. The effective bipolaron potential $U(z)$ as function of the relative electron coordinate $z = z_1 - z_2$ for $\eta = 0.2$. The results are shown for the Fourier series approach (solid curve) and for the best variational bipolaron wave function (dashed curve).

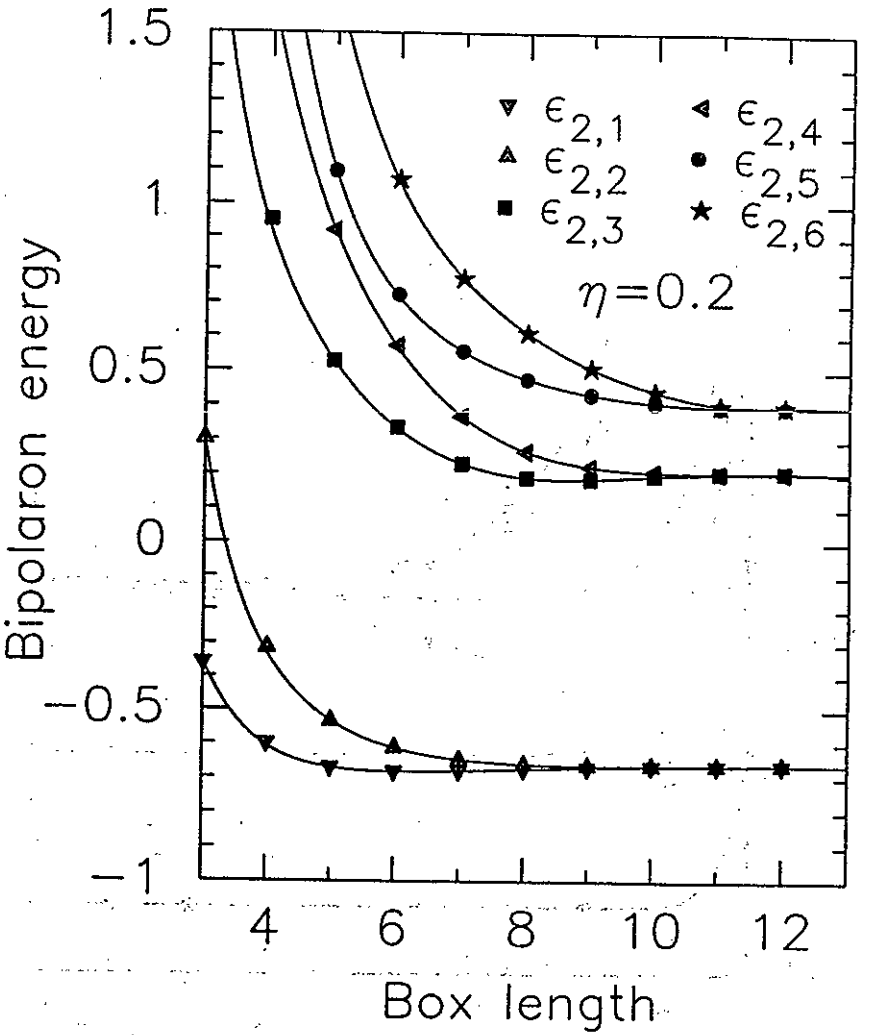

FIG. 11. The energy levels $\varepsilon_{2,n'}$ which belong to the states in the potential well generated by the first RES as function of the size of the confinement box (calculated with $N = M = 15$).

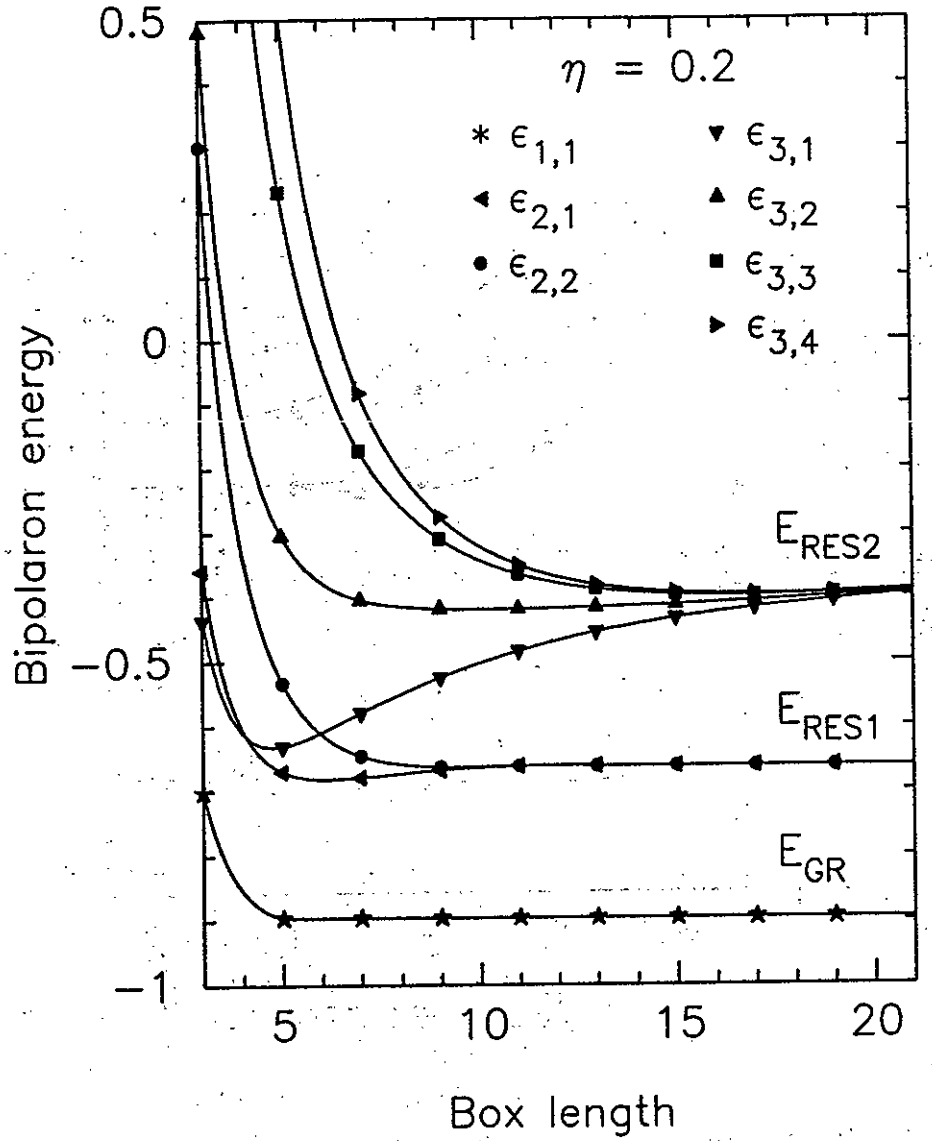

FIG. 12. The energy levels $\epsilon_{n,n'}$ for $n \leq 3$ and $n' \leq n+1$ ($n=3$) or $n' \leq n$ ($n=1,2$). For increasing box length $2L$ we observe a grouping of energy levels which is a consequence of the symmetry of the wave functions (calculated with $N = M = 15$).

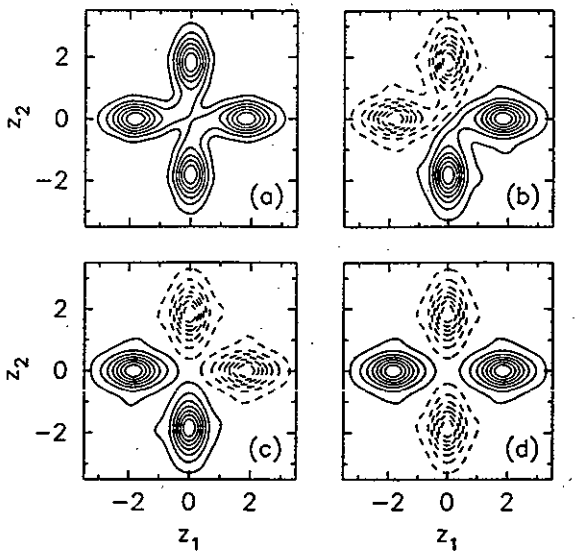

FIG. 13. The contourplots of the wave functions for $n = 3$ and $n' \leq 4$. The solid line corresponds to positive values of the wavefunction and the dashed line to negative values: a) $n' = 1$, b) $n' = 2$, c) $n' = 3$ and d) $n' = 4$.

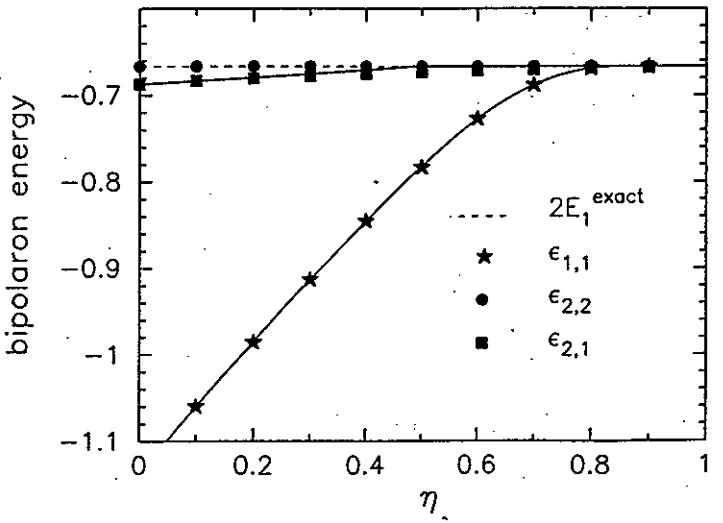

FIG. 14. The energies of the ground state, first RES and the ground state in the potential generated by this first RES as function of η (in the limit $N = M \to \infty$). The curves are guides to the eye.

REFERENCES

[1] V.L. Vinetskii, Zh. Eksp. Teor. Fiz. **40**, 1459 (1961) [Sov. Phys. JETP **13**, 1023 (1961)].

[2] V.K. Mukhomorov, Fiz. Tekh. Poluprovod. **16**, 1095 (1982) [Sov. Phys. Semicond. **16**, 700 (1982)].

[3] S.G. Suprun and B.Y. Moizhes, Fiz. Tverd. Tela **24**, 1571 (1982) [Sov. Phys. Solid State **24**, 1153 (1982)].

[4] J. Adamowski, Acta Phys. Pol. A **73**, 345 (1988); Phys. Rev. **B39**, 3649 (1989).

[5] F. Bassani, M. Geddo, G. Iadonisi, and D. Ninno, Phys. Rev. **B43**, 5296 (1991).

[6] G. Verbist, F. M. Peeters, and J. T. Devreese, Phys. Rev. **B43**, 2712 (1991).

[7] G. Verbist, M. A. Smondyrev, F. M. Peeters, and J. T. Devreese, Phys. Rev. **B45**, 5262 (1992).

[8] G. Verbist, F. M. Peeters, and J. T. Devreese, Solid State Commun. **76**, 1005 (1990).

[9] R. Micnas, J. Ranninger, and S. Robaszkiewicz, Rev. Mod. Phys. **62**, 43 (1990).

[10] A.S. Alexandrov, JETP Lett. **55**, 189 (1992)

[11] M. J. Rosseinsky, A. P. Ramirez, S. H. Glarum, D. W. Murphy, R. C. Haddon, A. F. Hebard, T. T. M. Palstra, A. R. Kortan, S. M. Zahurak, and A. V. Makhija, Phys. Rev. Lett. **66**, 2830 (1991).

[12] V.L. Vinetskii and E.A. Pashitskii, Ukrainskii Fiz. Zh. **20**, 338 (1975).

[13] D. Emin, Phys. Rev. Lett. **62**, 1544 (1989); D. Emin and M. S. Hillery, Phys. Rev. **B39**, 6575 (1989).

[14] K.-F. Berggren, T. J. Thornton, D. J. Newson, and M. Pepper, Phys. Rev. Lett. **57**, 1769 (1986).

[15] W. P. Su, J. R. Schrieffer, and A. J. Heeger, Phys. Rev. Lett. **42**, 1698 (1979).

[16] M. A. Smondyrev, E. A. Kochetov, G. Verbist, F. M. Peeters, and J. T. Devreese, Europhys. Lett., **19**, 519 (1992).

[17] E. Kartheuser, R. Evrard, and J. Devreese, Phys. Rev. Lett. **22**, 94 (1969); J.T. Devreese, in *Polarons in Ionic Crystals and Polar Semiconductors*, edited by J.T. Devreese (North-Holland Publishing Company, Amsterdam - London, 1972), p. 83; J. Devreese, J. De Sitter, and M. Goovaerts, Solid State Commun. **9**, 1383 (1971).

[18] F.M. Peeters and S.A. Jackson, Phys. Rev. **B31**, 7098 (1985); *ibid* **B34**, 1539 (1986).

[19] F. M. Peeters and M. A. Smondyrev, Phys. Rev. **B43**, 4920 (1991).

[20] F.M. Peeters, Wu Xiaoguang, and J.T. Devreese, Phys. Rev. **B33**, 3926 (1986).

[21] M. A. Smondyrev, F. M. Peeters, P. Vansant, and J. T. Devreese, to be published.

[22] E. P. Gross, Ann. Phys. (N.Y.) **99**, 1 (1976).

[23] H. Leschke and S. Wonneberger, J. Phys. **A22**, L1009 (1989); Corrigendum: J. Phys. **A23**, 1475 (1990).

[24] X. Wu, F. M. Peeters, and J. T. Devreese, Phys. Rev. **B31**, 3420 (1985).

[25] F. M. Peeters and J. T. Devreese, Phys. Rev. **B36**, 4442 (1987).

[26] M. A. Smondyrev, P. Vansant, F.M. Peeters, and J. T. Devreese, to be published.

Received by Publishing Department
on February 2, 1994.